

2018

Early Onset of Franciscan Subduction

Sean R. Mulcahy

Western Washington University, sean.mulcahy@wwu.edu

Jesslyn K. Starnes

Howard W. Day

Matthew A. Coble

Jeffrey D. Vervoort

Follow this and additional works at: https://cedar.wwu.edu/geology_facpubs



Part of the [Geology Commons](#)

Recommended Citation

Mulcahy, S. R., Starnes, J. K., Day, H. W., Coble, M. A., & Vervoort, J. D. (2018). Early onset of Franciscan subduction. *Tectonics*, 37, 1194–1209. <https://doi.org/10.1029/2017TC004753>

This Article is brought to you for free and open access by the Geology at Western CEDAR. It has been accepted for inclusion in Geology Faculty Publications by an authorized administrator of Western CEDAR. For more information, please contact westerncedar@wwu.edu.

Tectonics

RESEARCH ARTICLE

10.1029/2017TC004753

Key Points:

- Franciscan subduction began by about 180 Ma and continued as a single, long-lived, east dipping subduction zone for approximately 100 Ma
- The metamorphic history of high-grade blocks reflects several processes that operated at different times and places in the subduction zone
- Franciscan subduction is older than the Coast Range Ophiolite, which likely then formed above an east dipping Franciscan subduction zone

Supporting Information:

- Supporting Information S1
- Tables S1–S6

Correspondence to:

S. R. Mulcahy,
sean.mulcahy@wwwu.edu

Citation:

Mulcahy, S. R., Starnes, J. K., Day, H. W., Coble, M. A., & Vervoort, J. D. (2018). Early onset of Franciscan subduction. *Tectonics*, 37, 1194–1209. <https://doi.org/10.1029/2017TC004753>

Received 4 AUG 2017

Accepted 2 APR 2018

Accepted article online 19 APR 2018

Published online 5 MAY 2018

Early Onset of Franciscan Subduction

Sean R. Mulcahy¹ , Jesslyn K. Starnes^{2,3} , Howard W. Day², Matthew A. Coble⁴ , and Jeffrey D. Vervoort³

¹Geology Department, Western Washington University, Bellingham, WA, USA, ²Department of Earth and Planetary Sciences, University of California, Davis, CA, USA, ³School of the Environment, Washington State University, Pullman, WA, USA, ⁴Department of Geological Sciences, Stanford University, Stanford, CA, USA

Abstract The Franciscan subduction complex of California is considered a type example of a subduction-accretion system, yet the age of subduction initiation and relationship to the tectonic history of western North America remain controversial. Estimates for the timing of Franciscan subduction initiation are largely based either indirectly on regional tectonic arguments or from the ages of high-grade blocks within mélangé. Many of the high-grade blocks record counterclockwise pressure-temperature paths with early amphibolite overprinted by later eclogite and blueschist; however, their origin and significance with respect to subduction initiation have been debated. In contrast, some high-grade blocks show evidence for clockwise pressure-temperature paths and an early eclogite assemblage overprinted by later amphibolite. Zircon U-Pb ages from inclusions in garnet and Lu-Hf estimates of initial garnet growth ages from these samples record early eclogite metamorphism at ~176 Ma. Matrix zircon U-Pb ages and Lu-Hf estimates of final garnet growth ages record a barroisite-amphibolite assemblage overprint of eclogite at ~160 Ma. Combined with petrologic data and existing geochronology, the data suggest that (1) Franciscan subduction was underway by no later than 180 Ma, (2) continuous subduction metamorphism occurred for at least 100 Ma, and (3) Franciscan subduction initiation predated the formation of the overlying Coast Range Ophiolite, supporting models that form the ophiolite above an east dipping Franciscan subduction zone.

Plain Language Summary Subduction zones are places where dense ocean crust descends (or subducts) beneath more buoyant plates of continental or oceanic crust. Ancient subduction zones exposed at the Earth's surface provide important information on past plate movements and processes now occurring within active subduction zones. Determining the age that subduction began in ancient subduction zones is difficult because the earliest formed rocks are rarely preserved in the rock record. Our study focuses on the Franciscan Complex of California, which is considered a type example of an ancient subduction zone. The timing of Franciscan subduction initiation, however, has long been debated, resulting in conflicting models for the tectonic history of western North America. This study is unique because we dated the mineral zircon preserved as inclusions within garnet formed during the early stages of subduction. We also analyzed zircon outside of garnet formed during a younger event within the subduction history. The zircon inclusions within garnet yield an age of ~176 Ma, whereas the zircon outside the garnet had a younger age of ~160 Ma. These ages require that Franciscan subduction began by 180 Ma, significantly older than commonly believed and constrain models for the tectonic evolution of the western North American margin.

1. Introduction

Direct evidence for subduction initiation is often lacking because the earliest rocks are either lost to subduction or overprinted by later metamorphism and deformation. The Franciscan Complex of California (Figure 1) is considered a type example of a subduction-accretion system (Ernst, 1970), yet the age of subduction initiation and relationship to the tectonic history of western North America remain controversial. The Franciscan Complex is a Jurassic and Cretaceous assemblage of oceanic crust and sedimentary rocks deposited in or near the trench of the subduction zone beneath the Sierra Nevada batholith (Ernst, 1970; Hamilton, 1969). The Coast Range Ophiolite structurally overlies the Franciscan Complex and represents the oceanic basement on which the Great Valley Sequence was deposited (Bailey et al., 1970). The Great Valley Sequence (Figure 1) contains coeval sedimentary rocks that represent the fore-arc basin of the Sierra Nevada arc (Dickinson, 1970).

Current estimates for the onset of Franciscan subduction span approximately 30 Ma from 175 to 145 Ma. Platt (1975) recognized that high-grade blocks in mélangé might have formed as subduction began and early K-Ar

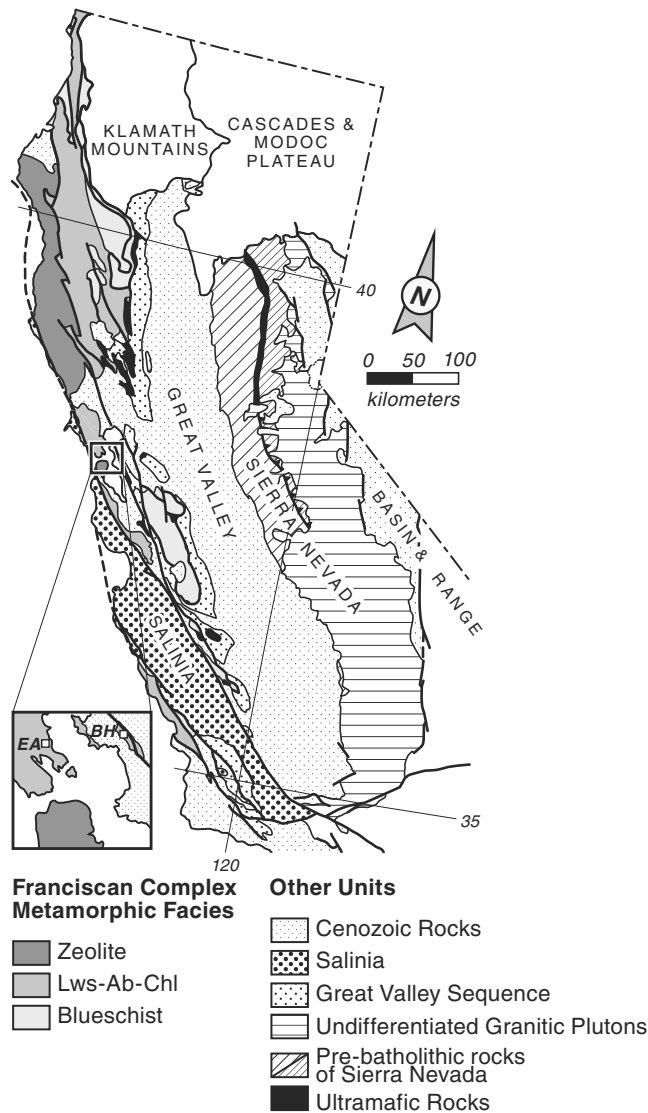


Figure 1. Simplified geologic map of California. Inset shows the locations of sample BH-32 (IGSN: IESRM0001), from the Berkeley Hills (37.9301, -122.2997), and sample EA (IGSN: IESRM0002), from the Tiburon Peninsula (37.9121, -122.4866). The Coast Range Ophiolite is marked by ultramafic rocks between the Franciscan Complex and the Great Valley Sequence. Modified after Day et al. (2003).

ages of these Franciscan metamorphic rocks ranged from 162 to 141 Ma (Coleman & Lanphere, 1971; McDowell et al., 1984; Mattinson, 1986). Cloos (1985) and Ukar et al. (2012) noted that garnet-blueschist and eclogite blocks yield K-Ar and $^{40}\text{Ar}/^{39}\text{Ar}$ ages between 155 and 145 Ma and interpreted the ages to record Franciscan subduction initiation at that time. In contrast, Anczkiewicz et al. (2004) argued that garnet-amphibolite formed during the earliest stages of subduction and interpreted a Lu-Hf garnet age from a single amphibolite sample to date subduction initiation circa 169 Ma. More recently, Ernst (2015) inferred that convergence began at 175 Ma based on the timing of early arc magmatism and terrane accretion in the Sierra Nevada and Klamath Mountains.

Ambiguity in the age of Franciscan subduction initiation has generated competing ideas about the origin of the Coast Range Ophiolite and the tectonic evolution of western North America. Debate over the tectonic setting of the Coast Range Ophiolite broadly falls into three models that interpret the ophiolite to have formed (1) during spreading in an east facing arc over a pre-Franciscan, west dipping subduction zone (Dickinson et al., 1996); (2) within a pre-Franciscan, oceanic spreading center that was drawn into a pre-Franciscan east dipping subduction zone (Hopson et al., 1996, 2008); and (3) during spreading in the fore arc of an east dipping Franciscan subduction zone (e.g., Godfrey & Klemperer, 1998; Stern & Bloomer, 1992; Saleeby, 1996). Early Franciscan metamorphic ages from high-grade blocks in mélangé overlapped with initial estimates for the formation of the Coast Range Ophiolite between 164 and 155 Ma (Lanphere et al., 1978) and led to the long-standing view that Franciscan subduction was coeval with the formation of the Coast Range Ophiolite. The wide range in more recent metamorphic ages and the uncertainty about which rocks are representative of subduction initiation permit the formation of the Coast Range Ophiolite before, after, or coeval with the onset of Franciscan subduction.

Direct evidence for the timing and nature of Franciscan metamorphism has come largely from high-grade blocks that record counterclockwise pressure-temperature paths and metamorphic ages that become younger as metamorphic grade decreases (Anczkiewicz et al., 2004; Wakabayashi & Dumitru, 2007). Although counterclockwise pressure-temperature paths are well documented from Franciscan exotic blocks (Krogh et al., 1994; Oh & Liou, 1990; Page et al., 2007; Tsujimori et al., 2006; Ukar & Cloos, 2014; Wakabayashi, 1990), early workers recognized eclogite overprinted by later amphibolite (Borg, 1956; Brothers, 1954; Switzer, 1945), suggesting that

some rocks experienced clockwise pressure-temperature paths. The different metamorphic histories recorded in these overprinted eclogites may therefore provide new and perhaps different information about the evolution of the Franciscan subduction complex.

We present new garnet and zircon radiometric ages from eclogite overprinted by amphibolite using garnet Lu-Hf and zircon U-Pb geochronology, respectively. Our results show that eclogite formed at approximately 176 Ma and was overprinted by amphibolite at circa 160 Ma, a time when many other amphibolites may have formed. The eclogite age is unambiguously related to subduction, and therefore, we suggest that Franciscan subduction began prior to 176 Ma. Published eclogite and amphibolite ages span much of the early subduction history and suggest that high-grade blocks are sampled from different depths and at different times within the subduction zone. Franciscan subduction began before the formation of the Coast Range Ophiolite, supporting models that favor the formation of the ophiolite within the fore arc of an east

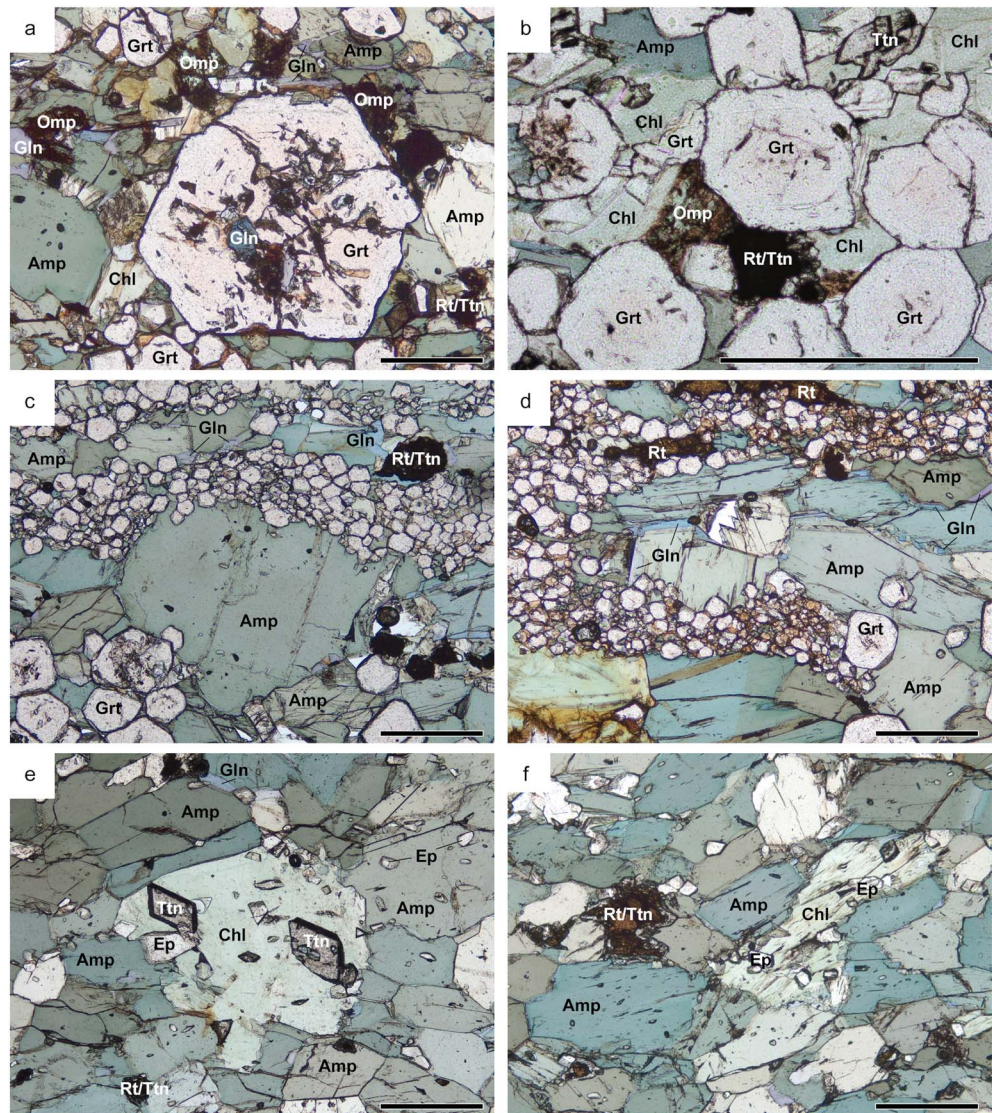


Figure 2. Mineral assemblages in sample BH-32 (IGSN: IESRM0001). (a) Garnet (Grt) porphyroblast and multiple omphacite (Omp) relics in a matrix of Na-Ca amphibole (Amp), (b) relic omphacite and partially resorbed garnet in a patch of late chlorite (Chl), (c) millimeter-scale garnet vein parallel the amphibole foliation, (d) garnet vein that locally crosscuts the foliation and Na-amphibole (Gln) rims on early Na-Ca amphibole, (e) late chlorite that cuts the foliation with euhedral titanite (Ttn), and (f) late chlorite with euhedral epidote, Na-Ca amphibole with subhedral inclusions of epidote (Ep), and titanite rims on rutile (Rt). Scale bar in each image is 0.5 mm.

dipping Franciscan subduction zone. When combined with published ages, the data suggest a single Franciscan subduction zone that was active for about 100 million years.

2. Sample Descriptions

We studied two plagioclase-free garnet amphibolites with evidence for an earlier eclogite assemblage (Figure 1) in order to determine if they record a different metamorphic history than high-grade blocks with a counterclockwise P-T trajectory. Both samples are from blocks in serpentinite matrix mélangé (Brothers, 1954; Bero, 2014) that structurally underlies serpentinitized peridotite and overlies the structurally highest Franciscan nappe in the San Francisco Bay region (Wakabayashi, 1992). Sample BH-32 (Figure 2) is from the Berkeley Hills and was originally described by Brothers (1954), who regarded the rock as an altered eclogite, and sample EA (Figure 3) is from the Tiburon Peninsula.

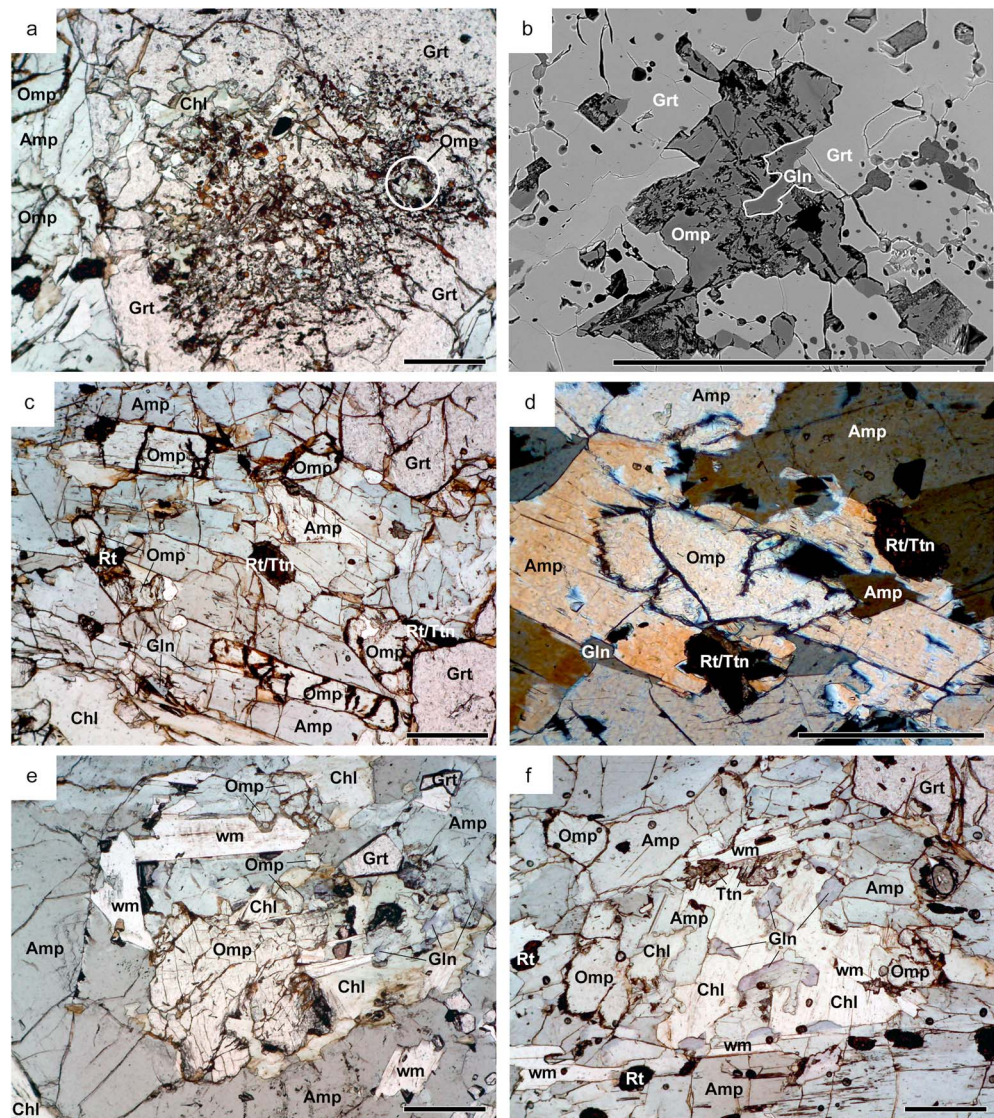


Figure 3. Mineral assemblages in sample EA (IGSN: IESRM0002). (a) Omphacite in the inclusion-filled core of garnet porphyroblast, (b) BSE image of the omphacite inclusion shown in (a) with omphacite that partially replaces glaucophane (outlined in white), (c) relict omphacite altered along grain boundaries and replaced by Na-Ca amphibole, (d) relict omphacite overgrown by Na-Ca amphibole (crossed-polarized light), and (e) omphacite associated with a patch of chlorite and white mica (wm). Note the fringes and patches of glaucophane associated with the patch. Most of the Na-Ca amphibole surrounding the omphacite is a single crystal, (f) relics of omphacite in a patch of Na-Ca amphibole, chlorite, white mica, titanite, and glaucophane. Scale bar in each image is 0.4 mm.

The samples share similar assemblages that consist of garnet porphyroblasts in a matrix of blue-green amphibole, rutile, and relict clinopyroxene (Figures 2 and 3). Garnet occurs as porphyroblasts with relatively inclusion-free rims and inclusion-rich cores (Figures 2a and 3a) and are variably resorbed and replaced by chlorite (Figure 2b) and amphibole. Clinopyroxene and glaucophane occur as inclusions within the garnet porphyroblasts (Figures 2a, 3a, and 3b). Garnet also occurs as fine euhedral grains in millimeter- to centimeter-scale veins that are parallel to and locally crosscut the amphibole foliation (Figures 2c and 2d). Within the matrix, clinopyroxene locally occurs in contact with garnet and amphibole but is altered to iron oxide along fractures and grain margins (Figures 2a, 2b, 3a, and 3c) and is variably overgrown or replaced by combinations of blue-green amphibole (Figure 3d), glaucophane, chlorite, white mica, and titanite. Clinopyroxene inclusions in garnet and relict clinopyroxene grains in the matrix are omphacite (Starnes, 2014; Figure S1 in the supporting information). Grains of blue-green amphibole, commonly barroisite and

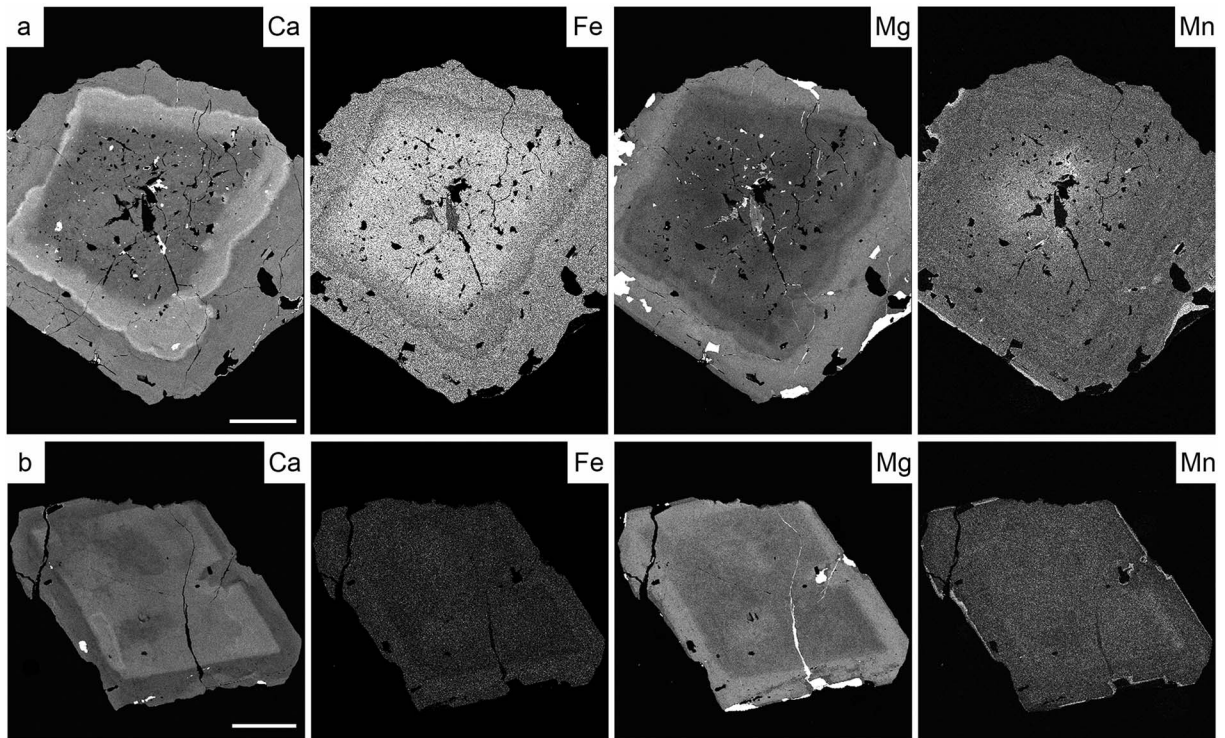


Figure 4. Qualitative, wavelength dispersive spectrometer elemental maps from garnet separates of sample EA (IGSN: IESRM0002). (a) More common zoning wherein the garnet core shows low Ca and Mg and high Fe and Mn relative to the surrounding mantle and (b) less common zoning wherein the garnet core shows high Ca and high Mn and low Fe and Mg relative to the surrounding mantle. Scale bar in (a) and (b) is 500 μm .

magnesiokatophorite (Leake et al., 1997), are overprinted by actinolite and locally rimmed and replaced by glaucophane (Figures 2, 3e, and S1; Starnes, 2014). Late chlorite occurs in patches with glaucophane (Figure 3f), euhedral to subhedral titanite (Figure 2e), and epidote (in sample BH-32; Figure 2f). Some white mica is intergrown with late chlorite but more commonly forms tabular books parallel to the foliation

Table 1
Isotopic Data for Garnet Lu-Hf Geochronology of Samples BH-32 (IGSN: IESRM0001) and EA (IGSN: IESRM0002)

Sample	Mineral	Lu (ppm)	Hf (ppm)	$^{176}\text{Lu}/^{177}\text{Hf}$	$^{176}\text{Hf}/^{177}\text{Hf}$	$\pm 2\sigma$
<i>Sample BH-32 (IGSN: IESRM0001)</i>						
Core age $\geq 171.5 \pm 0.9$ Ma; rim age $\leq 155.5 \pm 0.6$ Ma						
	Garnet	3.75	0.117	4.578	0.296074	10
	Garnet	3.73	0.123	4.315	0.296615	7
	Garnet	2.72	0.111	3.483	0.293396	9
	Garnet	2.60	0.126	2.932	0.291509	11
	Garnet	2.65	0.145	2.589	0.290865	7
	Garnet	2.41	0.139	2.457	0.289923	6
	Whole rock	0.195	4.63	0.0060	0.282793	4
	Whole rock	0.221	0.649	0.0484	0.282995	4
<i>Sample EA (IGSN: IESRM0002)</i>						
Core age $\geq 165.8 \pm 1.0$ Ma; rim age $\leq 154.6 \pm 0.9$ Ma						
	Garnet	2.16	0.141	2.176	0.289772	9
	Garnet	2.14	0.134	2.265	0.289577	6
	Garnet	2.52	0.153	2.345	0.290218	9
	Garnet	1.82	0.130	1.988	0.289048	7
	Garnet	1.95	0.130	2.120	0.289368	7
	Garnet	2.57	0.171	2.133	0.289496	5
	Whole rock	0.110	1.39	0.0112	0.283064	5
	Whole rock	0.105	0.324	0.0462	0.282981	6

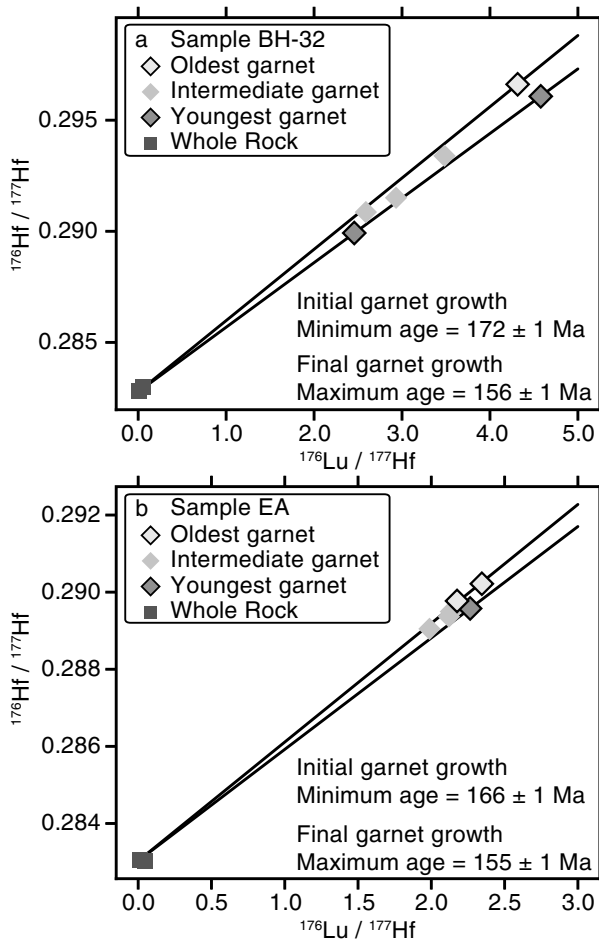


Figure 5. Garnet-whole-rock Lu-Hf isochrons. (a) Sample BH-32 (IGSN: IESRM0001) of the North Berkeley Hills and (b) sample EA (IGSN: IESRM0002) of the Tiburon Peninsula. Errors are reported as 2σ uncertainty and are smaller than the plotted symbols. In each isochron the minimum age for initial garnet growth is defined by the whole rock and oldest garnet separate(s) and the maximum ages for final garnet growth are defined by the whole rock and youngest garnet separate(s).

(Figure 3e). Apatite occurs as a late accessory phase, within garnetite veins, and as monomineralic veins in sample EA. Such monomineralic veins are commonly considered as evidence of fluid interaction (Bebout & Penniston-Dorland, 2016, and references within). Zircon is included in garnet and within matrix phases such as amphibole, chlorite, and rarely clinopyroxene.

In summary, the samples record evidence of an early eclogite assemblage overprinted by later amphibolite and blueschist assemblages. The presence of garnet and apatite veins and patches of chlorite, white mica, glaucophane, titanite, and epidote suggest one or more late fluid infiltration events. This metamorphic history contrasts with counter-clockwise metamorphic paths reported for other Franciscan blocks in which eclogite is more commonly retrograded to blueschist. We applied garnet Lu-Hf garnet geochronology to both samples and zircon U-Pb geochronology to sample EA from the Tiburon Peninsula to determine the ages of eclogite and amphibolite metamorphism.

3. Garnet Geochronology

3.1. Garnet Textures and Zoning

Textural relationships and chemical mapping suggest a complex garnet growth and resorption history. Garnet porphyroblasts mounted in epoxy exhibit variable zoning patterns (Figure 4). Some porphyroblasts preserve cores with low Ca and Mg and high Fe and Mn relative to the surrounding mantle (Figure 4a), whereas others preserve cores with high Ca and Mn and low Fe and Mg (Figure 4b). Garnet cores commonly display irregular and patchy zoning, and most garnets have a thin, distinct, outer rim with high Mn and Ca and low Mg. Between the patchy, zoned core and thin, outer rim, some garnets exhibit complex oscillatory zoning. The boundaries between compositional domains are commonly irregular or embayed and suggest multiple episodes of garnet resorption. Additional garnet compositions and elemental X-ray maps are provided in the supporting information (Figures S1–S3).

Garnetite veins in sample EA are compositionally zoned from the vein center to the vein edges with decreasing Mn, increasing Mg, and Fe that is highest at intermediate positions between the vein center and edges (supporting information Figure S4) and have compositions that at least partially overlap with the larger garnet porphyroblasts (Figure S1). Trace element zoning in garnet veins from the same block in Tiburon was interpreted to result from post-eclogite assemblage fluid infiltration (Cruz-Uribe & Feineman, 2009, 2010), and our observations suggest that the veins formed late during the amphibolite overprint.

3.2. Garnet Lu-Hf Geochronology

Garnet-whole rock Lu-Hf isochrons for both samples were determined at Washington State University following the procedure outlined by Mulcahy et al. (2014). Garnet veins were excluded from Lu-Hf dating by cutting vein-free material from the two samples. Garnet porphyroblasts were separated from the vein-free matrix by hand crushing, magnetic separation, and handpicking of individual grains. The concentrations of Lu and Hf were determined by isotope dilution, and uncertainties are estimated to be better than 0.5%. Uncertainties in $^{176}\text{Lu}/^{177}\text{Hf}$ for the purposes of regression and age calculations are estimated at 0.5%. Reported errors on $^{176}\text{Hf}/^{177}\text{Hf}$ represent within-run uncertainty expressed as 2σ standard error. Estimated total uncertainty on individual $^{176}\text{Hf}/^{177}\text{Hf}$ measurements for regressions and age calculations is estimated to be 0.01%. Ages were calculated with the ^{176}Lu decay constant values of Scherer et al. (2001) and Söderlund et al.

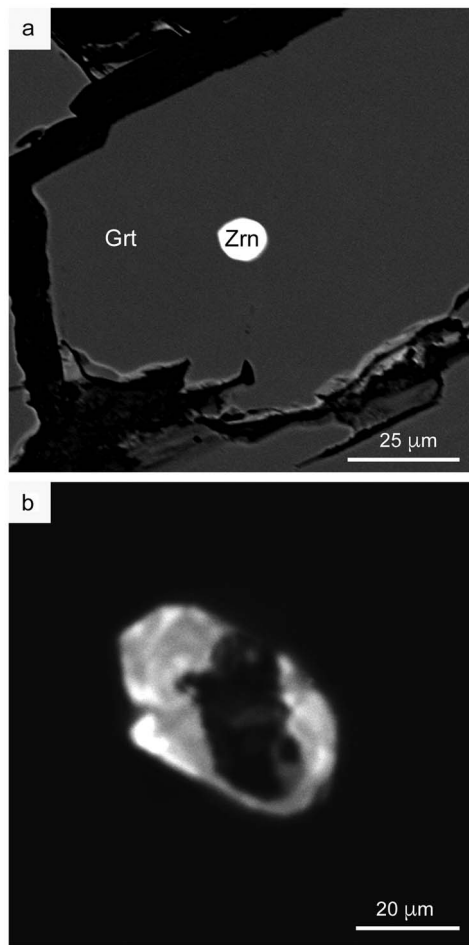


Figure 6. Representative zircon morphology from sample EA (IGSN: IESRM0002). (a) BSE image of a rounded, anhedral zircon (Zrn) included in garnet (Grt) and (b) CL image of subhedral zircon separated from the matrix with a CL dark core and CL bright rim.

and cathodoluminescences (CL) and the maximum dimension of zircon ranges from $<5 \mu\text{m}$ to $50 \mu\text{m}$ but commonly is about $15 \mu\text{m}$. Zircon inclusions in garnet are most commonly rounded, equant grains (Figure 6a), and subhedral grains with one or two recognizable crystal faces are rare. Zircon in garnet was generally too small ($\leq 20 \mu\text{m}$) to obtain high-quality CL images or identifiable textures. Zircon recovered from the matrix is typically larger than inclusions in garnet and is anhedral or subhedral (Figure 6b). CL imaging shows that most grains have dark interiors and bright overgrowths, but distinct “cores” and “rims” commonly cannot be distinguished reliably (Figure 6b and supporting information Figure S5).

Supporting information Figure S3 illustrates the location of each analyzed zircon inclusion within its host garnet porphyroblast and chemical zoning maps of the garnet host. Zircon inclusions in garnet mostly occur within the patchy, zoned interiors, and none were observed in the centers of garnet grains. Less commonly, zircon inclusions occur on the boundaries between garnet compositional domains and even fewer occur near late garnet rims.

4.2. Zircon U-Pb Geochronology

Zircon $^{206}\text{Pb}/^{238}\text{U}$ ages were determined using the Stanford-USGS SHRIMP-RG (sensitive high-resolution ion microprobe with reverse geometry). Zircon inclusions in garnet were analyzed in an attempt to date the early eclogite assemblage, and zircon grains in the matrix were analyzed to date the younger amphibolite assemblage. Individual dates included in weighted mean ages are listed in Table 2, and detailed analytical methods

(2004) and are reported with the associated 95% confidence interval. Concentration and isotopic data for garnet Lu-Hf isochrons are listed in Table 1.

Six garnet separates analyzed from each sample show considerable scatter that we interpret to reflect variable mixing of complexly zoned cores and rims within each garnet fraction (Figure 5). Sample BH-32 produced a two-point isochron age for the oldest garnet separate of $172 \pm 1 \text{ Ma}$ and a three-point isochron for the youngest garnet separate of $156 \pm 1 \text{ Ma}$ (Figure 5a). Sample EA produced a three-point isochron age for the oldest garnet separates of $166 \pm 1 \text{ Ma}$ and a two-point isochron for the youngest garnet separate of $155 \pm 1 \text{ Ma}$ (Figure 5b). Two and three-point isochrons likely underestimate the true uncertainty (Ludwig, 2009; Wendt & Carl, 1991), and we therefore regard these ages as approximate estimates for the timing of garnet rim and core growth. In this interpretation, because the oldest fractions may be mixed populations, they yield minimum estimates for initial garnet growth at $\geq 166\text{--}172 \text{ Ma}$. Likewise, because the youngest fractions may also be mixed, they yield maximum estimates for the late garnet growth at $\leq 155\text{--}156 \text{ Ma}$. Because omphacite locally occurs as inclusions within garnet cores (Figures 3a and 3d), we associate the $\geq 172\text{--}166 \text{ Ma}$ ages with eclogite facies metamorphism. Likewise, because subhedral or euhedral garnet rims commonly appear to be in textural equilibrium with the Na-Ca amphibole, we associate the $\leq 156\text{--}155 \text{ Ma}$ ages with the amphibolite overprint. The garnet ages, therefore, suggest eclogite metamorphism early in the Franciscan subduction history followed by a younger amphibolite overprint. To test this hypothesis further and to date the ages of the eclogite assemblage and amphibolite overprint more accurately, we determined U-Pb ages of zircon inclusions within garnet and zircon in the matrix assemblage of sample EA.

4. Zircon Geochronology and Geochemistry

4.1. Zircon Occurrence

Zircon in sample EA typically occurs as small ($\leq 50 \mu\text{m}$) inclusions within both garnet porphyroblasts and the matrix mineral assemblage. Zircon grains were imaged with backscattered electrons (BSE)

Table 2
Individual ^{206}Pb - ^{238}U Zircon Ages From Sample EA (IGSN: IESRM0002) Used in the Weighted Mean Ages of Figure 7

Analysis	Age (Ma)	$\pm 2\sigma$
<i>Zircon within garnet</i>		
JSEA1-1.2	177	4
JSEA1-1-5.1	181	2
JSEA1-1-8	171	5
JSEA1-1-8-2	175	3
JSEA1-1-9.2	208	9
JSEA1-1-13.1	177	4
JSEA1-1-13.2	176	2
JSEA1-1-14	170	7
JSEA1-2-5.1	168	5
JSEA1-2-11	196	7
JSEA1-2-16	182	3
JSEA2-3-1	175	6
JSEA2-3-2	161	5
JSEA2-3-9	163	3
JSEA2-3-16.2	164	5
JSEA2-4-5	169	7
JSEA2-4-7.1	183	4
JSEA2-5-1.1	177	5
JSEA2-6-5.1	201	12
<i>Zircon within matrix minerals</i>		
JSEA4-1.1	150	7
JSEA4-2.1	156	5
JSEA4-2.2	165	2
JSEA4-3.1	144	6
JSEA4-6.1	161	2
JSEA4-6.2	168	5
JSEA4-8.1	148	7
JSEA4-8.2	162	6
JSEA4-9.1	161	8
JSEA4-9.2	160	4
JSEA4-10.1	148	5
JSEA4-11.1	144	10
JSEA4-12.1	154	4
JSEA4-12.2	155	2
JSEA4-13.1	133	6
JSEA4-14.1	165	2
JSEA4-14.2	159	3
JSEA4-16.1	166	3

and expanded zircon data are in the supporting information (Table S1). The data presented in these tables are unique in two respects. First, we examined over 100 handpicked garnet porphyroblasts in sample EA in order to identify inclusions of zircon suitable for analysis in situ. We made in situ analyses of 29 small zircon inclusions with maximum dimensions commonly about 20 μm and calculated the weighted mean age of 19 of those analyses (Table 2). Second, we compare those results directly with analyses of zircon from the matrix of the same sample (Table 2). We concentrated that zircon by traditional means from matrix material from which all garnet had been removed. We mounted about 5 mg of a fraction containing titanite, rutile, and other minerals and identified the rare zircon grains using BSE and CL imaging. We made 24 analyses and calculated the weighted mean age of 18 analyses from 12 grains identified in this way (Table 2).

The ages are reported as calculated intercept ages on inverse concordia plots and as weighted mean $^{206}\text{Pb}/^{238}\text{U}$ ages (Figure 7). All uncertainties are reported at 2σ (standard error). The average uncertainty for individual zircon dates was 4.6% for all analyses, with uncertainty generally increasing with decreasing U concentrations and/or decreasing radiogenic Pb. The weighted mean ages are the preferred ages, and the quoted uncertainties include measurement error (internal) and uncertainty propagated from the scatter in the standard calibrations. For both matrix and garnet zircon, the mean square of weighted deviates (MSWD) is higher than would be expected for a single population (critical MSWD for $n = 19$ ranged from 0.45 to 1.75; Mahon, 1996); therefore, reported 2σ standard errors were multiplied by the square root of the MSWD to reflect this additional scatter. We attribute some of the excess scatter in zircon analyses to low analytical precision of U-poor zircons. The youngest and oldest calculated ages are predominantly zircon grains with <15 ppm U (supporting information Table S1).

Zircon inclusions within garnet yield a calculated intercept age of 176.5 ± 3.8 Ma (MSWD 4.4; Figures 7a and 7b) and a weighted mean age of 175.6 ± 4.1 Ma (MSWD = 4.3; Figure 7c). Zircon in the matrix has an intercept age of 160.3 ± 3.2 Ma (MSWD = 3.5; Figures 7d and 7e) and weighted mean age of 159.5 ± 4.2 Ma (MSWD = 4.2; Figure 7f). The 2σ uncertainties of the two weighted mean ages do not overlap and therefore are statistically distinguishable. Although both samples have high a MSWD, elimination of obvious older or younger grains improves the fit (decreases the MSWD) but has no significant impact

on the estimated ages because the uncertainties of those grains are large, and their influence on the weighted mean age is small.

4.3. Zircon Trace Element Geochemistry

To better relate the zircon U-Pb ages to the early eclogite and late amphibolite overprint, we measured the trace element compositions of both zircon populations in situ with SHRIMP-RG. Analytical methods and results are given in the supporting information (Table S2). Zircon inclusions in garnet have low Th/U (~ 0.02 ; Figure 8a), a minimal Eu anomaly (~ 0.82 ; Figure 8b), low total heavy rare earth element (REE) concentrations (Figure 8c), and shallow positive or negative slopes from middle to heavy REE concentrations (Figures 8d and 8e). In contrast, matrix zircon has generally higher Th/U (~ 0.39 ; Figure 8a), an elevated and variable Eu anomaly (~ 3.21 ; Figure 8b), high total heavy REE concentrations (Figure 8c), and steep positive slopes from middle to heavy REE concentrations (Figures 8d and 8f). Trace element concentrations correlate with age, and while there is some compositional overlap between the zircon populations, the oldest zircon grains in garnet are chemically distinct from the youngest zircon grains in the matrix assemblage.

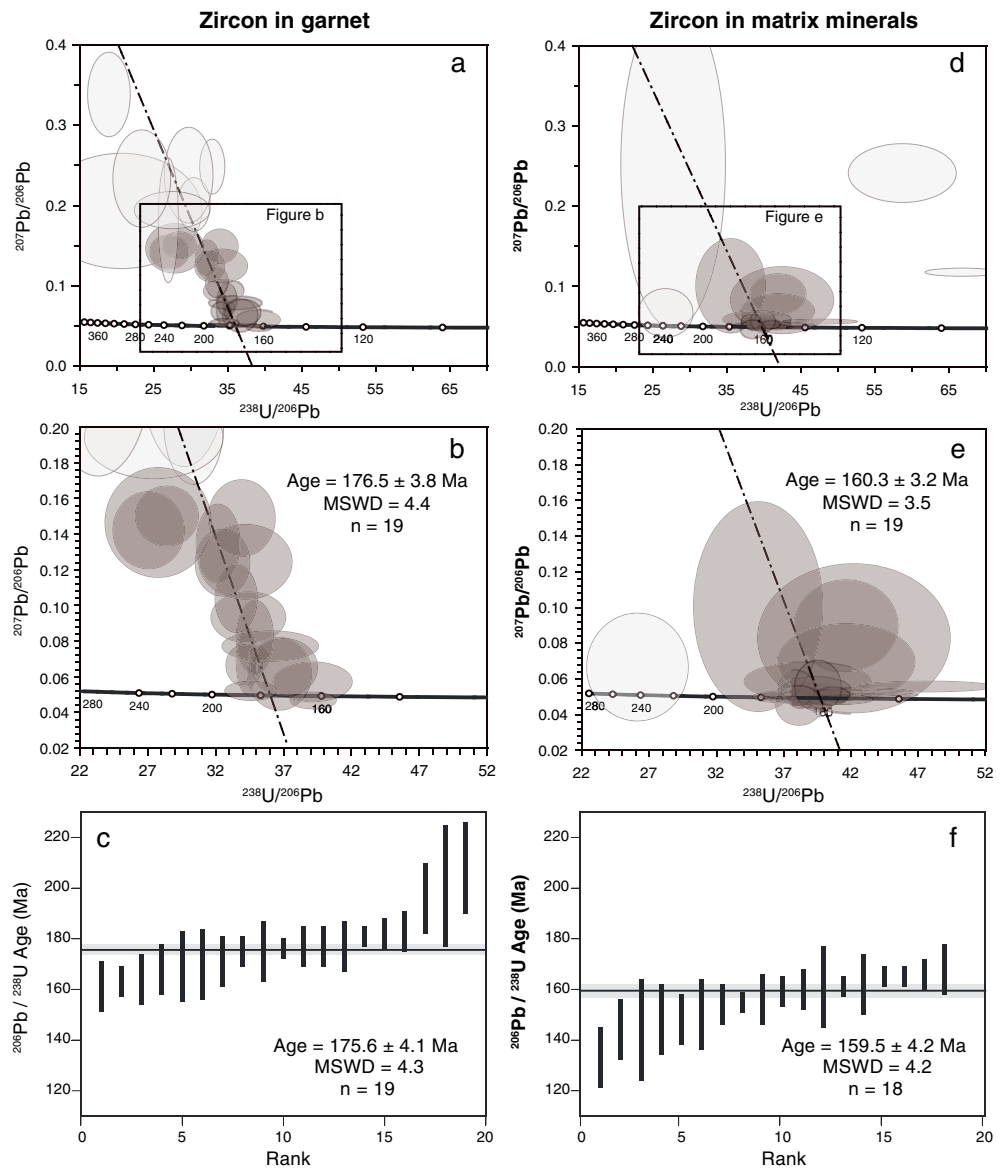


Figure 7. Zircon U-Pb SHRIMP ages from sample EA (IGSN: IESRM0002). (a) Inverse concordia diagram for zircon in garnet, (b) enlarged area shown in (a), (c) weighted average ^{207}Pb -corrected $^{206}\text{Pb}/^{238}\text{U}$ age of zircon in garnet, (d) inverse concordia diagram for zircon in matrix minerals, (e) enlarged area shown in (d), and (f) weighted average age of zircon in matrix minerals. Calculated intercept ages are fixed to $^{207}\text{Pb}/^{206}\text{Pb} = 0.846 \pm 0.001$. Light grey error ellipses represent individual analyses that were excluded from the calculated age. Error ellipses are 2σ . Error bars in the weighted averages are shown at 2σ , and the error in the weighted mean is reported as the 95% confidence interval, including the standard calibration error.

5. Discussion

The composite metamorphic history of the samples in this study preserves an apparent clockwise pressure-temperature path, consistent with the observations of early workers (Borg, 1956; Brothers, 1954; Switzer, 1945) and distinct from the counterclockwise pressure-temperature path documented in other high-grade blocks (Krogh et al., 1994; Page et al., 2007; Tsujimori et al., 2006; Ukar & Cloos, 2014; Wakabayashi, 1990). The mineral assemblages record a three-stage metamorphic evolution of early eclogite metamorphism, an intermediate barroisite-amphibolite overprint, and late blueschist assemblages. The early eclogite assemblage is preserved as omphacite and rutile inclusions in garnet cores, omphacite inclusions in Na-Ca amphibole, and relict omphacite in the matrix. The eclogite assemblage was overprinted by an amphibolite

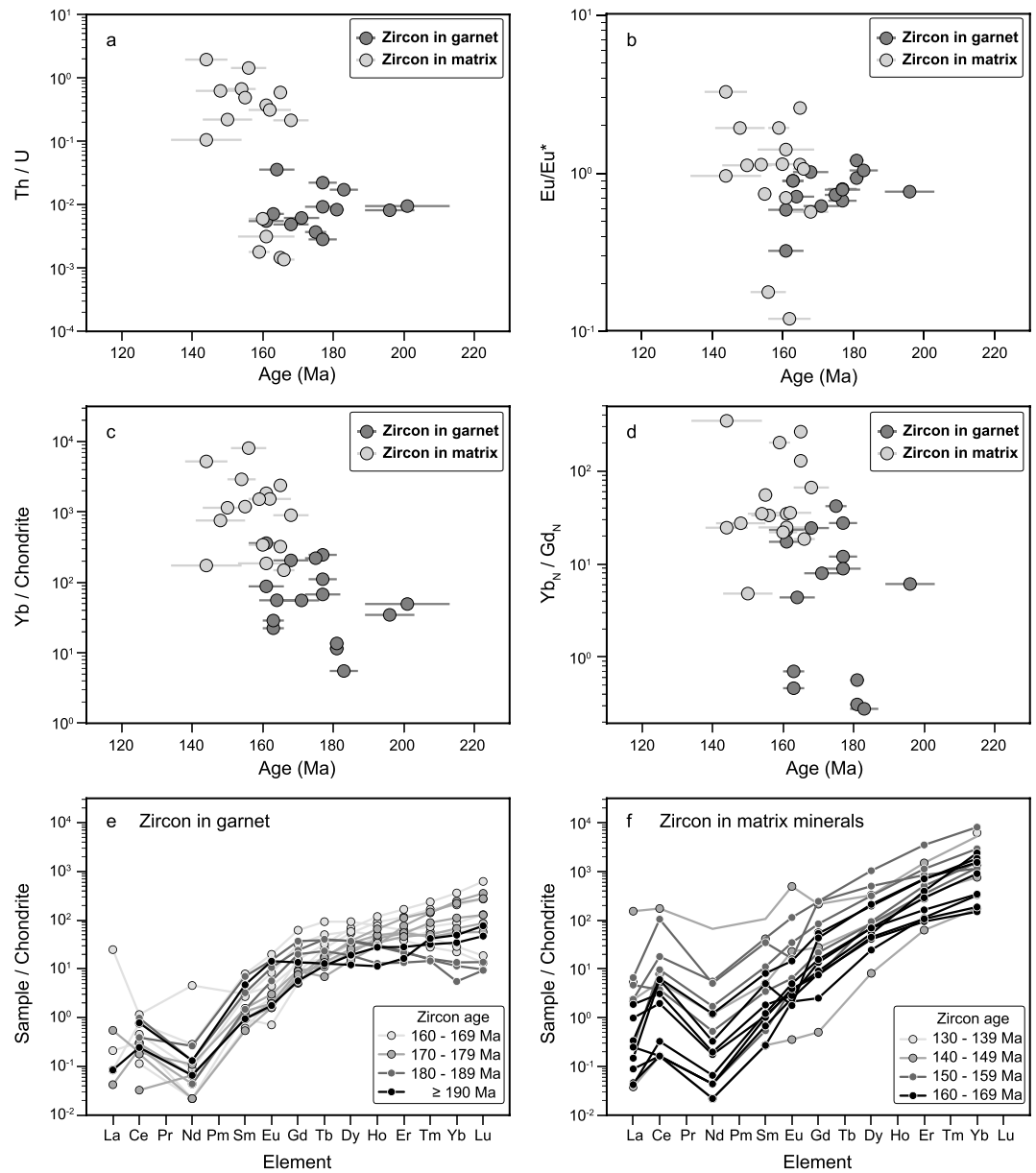


Figure 8. Zircon trace element composition versus $^{206}\text{Pb}/^{238}\text{U}$ age for sample EA (IGSN: IESRM0002). (a) Th/U ratio. (b) Eu anomaly. $\text{Eu}/\text{Eu}^* = \text{Eu}_N/[(\text{Sm}_N \times \text{Gd}_N)^{0.5}]$. (c) Yb/chondrite. Normalized Yb is used as a proxy for HREE. (d) Yb_N/Gd_N . The chondrite-normalized ratio is used as a proxy for slope from MREE to HREE. (e and f) Chondrite-normalized REE diagrams for zircon inclusions in garnet and matrix minerals, respectively. Chondrite normalization values are from McDonough and Sun (1995).

assemblage of inclusion-free garnet rims, Na-Ca amphibole, white mica, rutile, and possibly epidote. The late blueschist assemblage is characterized by Na-amphibole, chlorite, white mica, titanite, and epidote. The fact that garnetite veins, which are associated with apatite veins, locally cut the amphibole foliation (Figure 2) suggests that they formed during or later than the amphibolite overprint.

Zircon U-Pb ages date the timing of the eclogite phase of metamorphism and the amphibolite overprint at 176 ± 4 Ma and 160 ± 4 Ma, respectively. Although there is overlap of individual dates from inclusions in garnet and matrix zircon, the presence of two distinct populations is supported by several observations. First, the mean ages of the two populations differ by twice the value of the combined 95% confidence intervals. Second, a Kolmogorov-Smirnov (K-S) test indicates that the two populations are statistically distinct (supporting information Figure S6). This test is used when two populations are not normally distributed or if

their distributions are unknown (Conover, 1971; Daniel, 1990). In this case, the critical value of the D statistic describing these populations considerably exceeds the value required to conclude that the populations are different at the 0.01 level of significance. Third, although they are complicated by the complex garnet growth and resorption history, the Lu-Hf ages combined with petrographic observations suggest initial garnet growth at eclogite conditions, followed by multiple episodes of growth and resorption, and final garnet growth during the amphibolite overprint occurred over a prolonged period (≥ 10 –15 Ma). Finally, the trace element compositions of the zircon in the two populations are distinctly different.

The trace element compositions of zircon in garnet have low Th/U, minimal Eu/Eu^{*}, low total REE concentrations, and flat to negative heavy rare earth element (HREE) profiles that are consistent with having formed at eclogite conditions (Rubatto, 2002; Skublov et al., 2012). In contrast, the trace element chemistry of matrix zircon has elevated and variable Th/U, Eu/Eu^{*}, and REE concentrations that may reflect trace element enrichment with progressive hydration of the early eclogite assemblage. The change in trace element chemistry between compositionally distinct oldest and youngest zircons is transitional and suggests that zircon grew and responded to changing physical and chemical conditions throughout the complex metamorphic history of the sample. Sorensen and Grossman (1989) documented metasomatic enrichment of Franciscan amphibolite that preserved evidence of an earlier eclogite assemblage, and Page et al. (2013) interpreted similar zircon trace element compositions in Franciscan high-grade blocks to reflect zircon growth during garnet resorption or through interaction with an external REE source.

Although most of the zircons have resolvable interior and rim zones visible in CL (supporting information Figure S5), we find no evidence that the older ages represent protolith ages in either the zircon inclusions in garnet or the zircon recovered from the matrix. Many, if not most, zircon grains in garnet are small compared to the size of the ion beam. Consequently, most spot analyses contain contributions from interior and rim zones. Beam placements within the zircon grains were documented using BSE images after analysis. For small zircon grains that occurred as inclusions within garnet, we attempted to minimize overlap onto the host garnet, which may contribute common Pb to the analysis, by moving the beam to maximize $^{90}\text{Zr}_2^{16}\text{O}$ counts. There was no observed correlation between the beam placement and the apparent age of the zircon (supporting information Table S2).

Six different grains from the matrix sample were large enough that we successfully placed two analyses on the polished surface. We found no statistical differences between multiple ages obtained on a single zircon grain. Although brighter CL exteriors are commonly slightly younger than the CL-dark zircon interior, there is no consistent correlation between age and amount of CL-bright rim material analyzed within analytical resolution (supporting information Figure S5). Consequently, we conclude that there is no evidence that cores of zircon grains are significantly older than the rims or that they influenced the dispersion of ages observed.

Within each age population of zircon there is dispersion of ages that leads to slight overlap of the individual grains from each sample. The ages of zircon inclusions in garnet range from 208 ± 18 Ma to 161 ± 10 Ma (2σ), and the difference of 47 ± 21 Ma appears to be real. Likewise, the range in ages of matrix zircon from 168 ± 10 Ma to 133 ± 12 Ma also appears to be real because the difference is 35 ± 16 Ma. The dispersion of the two populations in sample EA suggests that zircon was growing or responding to metamorphic processes throughout a prolonged and chemically dynamic history but does not detract from the conclusion that garnet preserves much older zircon than the matrix.

The new ages presented here together with published Franciscan geochronology imply that Franciscan subduction began by no later than about 180 Ma, assuming that eclogite formed following the first few million years of subduction (e.g., Gerya et al., 2002). Eclogite metamorphism at 176 ± 4 Ma provides the first *direct* evidence that the Franciscan subduction zone was active in the Early Jurassic, 10–20 million years before many estimates for the onset of subduction (e.g., Anczkiewicz et al., 2004; Cloos, 1985; McDowell et al., 1984; Ukar, 2012). This is consistent with previously published, but possibly suspect, mineral ages from metamorphic rocks distributed throughout the Franciscan and with indirect evidence. Firsov and Dobretsov (1970) reported a K-Ar clinopyroxene age of 175 ± 4 from eclogite. Suppe and Foland (1978) reported Rb-Sr mineral-whole-rock isochrons of 180 Ma in metachert, to which the authors first ascribed no age significance and then conceded the possibility the ages were geologically significant. In abstracts, Ross and Sharp (1986) reported a garnet Sm-Nd age of 190 ± 10 Ma from garnet amphibolite, and Page et al. (2003) reported a zircon U-Pb age of 178 ± 7 from eclogite. *Indirect* evidence for early onset of Franciscan subduction is supplied by

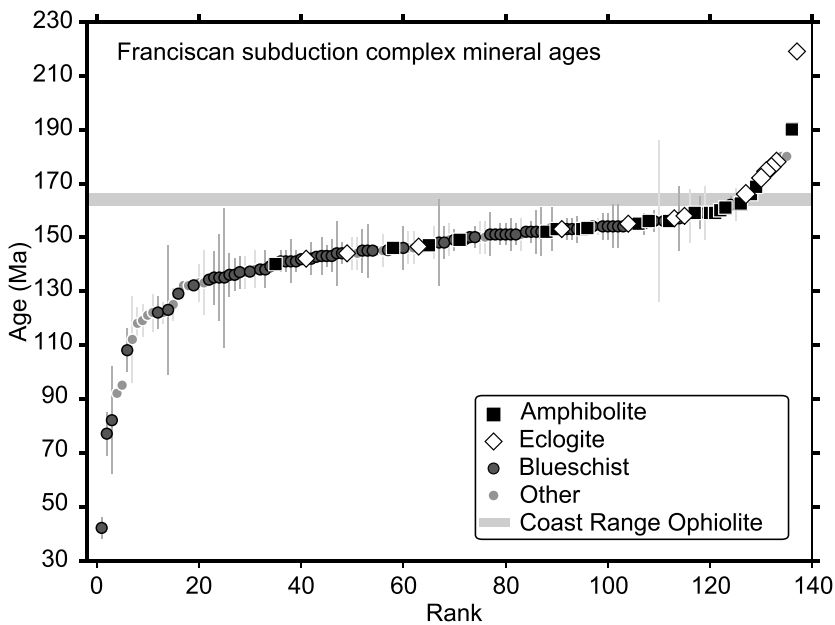


Figure 9. Published Franciscan ages versus ranked age from youngest to oldest. The grey horizontal bar depicts the best estimate for the age of the Coast Range Ophiolite. Amphibolite and eclogite symbols are emphasized for clarity. Error bars are plotted as 2σ . The data and discussion of published ages are provided in the supporting information.

convergence along the western North American inferred on the basis of 180–170-Ma arc magmatism and Early Jurassic terrane accretion in the Sierra Nevada and Klamath Mountains (Day & Bickford, 2004; Ernst, 2015; Fagan et al., 2001; Hacker, 1993; Wright & Fahan, 1988) and by Shervais et al. (2005) based on Middle Jurassic ages derived from the Coast Range Ophiolite.

The distribution of published ages implies that Franciscan metamorphism was continuous and long lived (Figures 9 and S7). The combined mineral and isochron ages extend from 180 Ma to 72 Ma. Most of the data define a homogeneous population with an essentially uniform slope that spans 162 Ma to 125 Ma. The younger limit of this population corresponds closely to a proposed change in the Franciscan subduction regime at circa 123 Ma (Dumitru et al., 2010), whereas the upper limit is similar to the time of eclogite alteration to amphibolite proposed for sample EA. Eclogite and amphibolite ages occur throughout the first 35–40 Ma of subduction, and exotic blueschist blocks are dated as early as ~160 Ma and extend to younger than 130 Ma. The youngest Franciscan metamorphic ages are constrained by jadeite-bearing metasedimentary rocks from the Diablo range that were deposited at

<85 Ma (Joesten et al., 2004) and were exhumed between 68 and 54 Ma (Tripathy et al., 2005; Unruh et al., 2007). Rocks in the Franciscan subduction zone therefore record approximately 100 million years of continuous metamorphism.

Dumitru et al. (2010) presented a detailed, critical reassessment of whole-rock argon ages and concluded that these early ages were best excluded from further studies. We do not disagree with their assessment but suggest that the distribution of the whole rock ages is consistent with the known times of subduction and exhumation processes in the Franciscan Complex. Whole-rock argon ages were excluded from Figure 9 but are presented in the supporting information (Figure S8 and Table S3; Awalt et al., 2013; Catlos & Sorensen, 2003; Dalrymple, 1979; Evarts et al., 1992; Fritz, 1975; Keith & Coleman, 1968; Lanphere, 1971; Lee et al., 1964; Mankinen et al., 1991; Mattinson & Echeverria, 1980; Mattinson & Hill, 1976; McLaughlin & Ohlin, 1984; Moore & Blake, 1989; Mulcahy et al., 2009; Peterman et al., 1967; Ross & Sharp, 1988; Suppe, 1969; Suppe & Armstrong, 1972; Wakabayashi & Deino, 1989). The principal effects of including the whole-rock data would be to extend the lower limit of the homogeneously distributed population from 125 Ma to 103 Ma and to enhance the definition of a subsidiary population ranging from 103 to 72 Ma.

The common occurrence of low-temperature blueschist overprints on earlier higher-temperature eclogite and amphibolite assemblages has commonly been ascribed to secular cooling of the subduction zone following subduction initiation (e.g., Krogh et al., 1994; Platt, 1975; Wakabayashi, 1990). Anczkiewicz et al. (2004) interpreted a series of Lu-Hf garnet ages that decreased with metamorphic grade to reflect prolonged cooling from initial high-grade conditions. In contrast, Page et al. (2007) argued that high-grade blocks could have formed throughout the subduction history and do not necessarily share a common origin. This argument is supported by the presence of eclogite and amphibolite high-grade blocks that formed throughout much of the early Franciscan subduction history, rather than at just the initiation of subduction (Figure 9). A third possibility is that the complex metamorphic history of sample EA reflects the circulation and exhumation of blocks within a serpentized layer above or within the subduction channel (e.g., Gerya et al., 2002). Determining the relative contribution of each of these processes may require that the ages of protolith, peak metamorphism, and subsequent cooling be tied to detailed pressure-temperature paths of individual blocks within the mélange. However, the record of multiple metamorphic events preserved in sample EA is, perhaps, most consistent with the latter two interpretations.

Early onset of Franciscan subduction likely predates the formation of the Coast Range Ophiolite (Figure 9). The most precise and reliable ages for the Coast Range Ophiolite are four zircon U-Pb ages from plagiogranites determined by chemical abrasion-thermal ionization mass spectrometry (CA-TIMS; Hopson et al., 2008; Mattinson & Hopson, 2008) and four Ar-Ar analyses of glass from hyaloclastites in the Stonyford volcanic complex (Shervais et al., 2005). The zircon analyses range from 165.6 ± 0.4 Ma to 161.1 ± 0.1 Ma, and the glass samples cluster tightly in the range 164.6 ± 0.7 Ma to 163.8 ± 0.8 Ma (supporting information Figure S9). Considering all sources of error including uncertainties in decay constants, the U-Pb and Ar-Ar apparent ages are indistinguishable (Shervais et al., 2005). Hopson et al. (1981) interpreted the plagiogranites as late in the ophiolite evolution, and Shervais et al. (2005) suggested that the ophiolite formation was complete before or during the eruption of the Stonyford volcanic complex. On this basis, the age of earliest Franciscan eclogite and amphibolite metamorphism predates these most reliable ages for the Coast Range Ophiolite.

The oldest ages from the Coast Range Ophiolite are also younger than the 176 Ma or older metamorphism within the Franciscan Complex. Zircon from a plagiogranite that intrudes sheeted dikes yielded a U-Pb upper intercept age of 169.7 ± 4.1 Ma (2σ), and slightly discordant zircon fractions from a quartz diorite sill did not produce a reliable upper intercept, but the crystallization age was considered to be 172.0 ± 4.0 Ma (Shervais et al., 2005). The quartz diorite sill was interpreted as part of a suite of diorites that postdates all earlier, ultramafic, and gabbroic intrusions in the ophiolite (Shervais et al., 2005). Although we have only a one-sided constraint on the time at which construction of the Coast Range Ophiolite began, the available evidence suggests that subduction metamorphism was under way before the inception of the ophiolite.

The best ages for the Coast Range Ophiolite indicate that the formation of the ophiolite was not complete for ≥ 20 million years after the start of Franciscan subduction. The older age of Franciscan subduction supports the formation of the ophiolite within a Franciscan suprasubduction zone setting (e.g., Stern & Bloomer, 1992; Saleeby, 1996; Shervais et al., 2005). Other models for the tectonic setting of the ophiolite, within either a pre-Franciscan east facing arc or mid-ocean ridge spreading center, predict that the Coast Range Ophiolite is older than Franciscan subduction and are therefore incompatible with the observed ages. Formation of the Coast Range Ophiolite in an east facing arc requires that the ophiolite formed over a west dipping subduction zone followed by a reversal of subduction polarity as a younger, east dipping, Franciscan subduction zone was established (e.g., Ingersoll & Schweickert, 1986). Formation of the Coast Range Ophiolite at a mid-ocean ridge requires a separate, pre-Franciscan subduction zone to draw the ophiolite to the continental margin before Franciscan subduction began outboard of the ophiolite (e.g., Hopson et al., 2008). Both hypotheses require that high-grade blocks older than the ophiolite would be products of this earlier subduction zone that were then incorporated and exhumed within the later Franciscan subduction zone. The metamorphic ages with the Franciscan Complex (Figure 9), however, are continuous and uninterrupted before, during, and after the formation of the Coast Range Ophiolite. The uninterrupted record of subduction metamorphism over approximately 100 Ma suggests that the Franciscan was a single, long-lived, east dipping subduction zone.

Zircon ages within a single sample record two discrete metamorphic events that together span much of the early Franciscan evolution, similar to the ages of eclogite and amphibolite high-grade blocks. Any given sample within the continuous distribution of Franciscan ages provides a snapshot of the subduction history at that time. The zircon age population within sample EA would appear to be unique in recording two separate episodes of metamorphism within a single sample. In addition, although zircon ages within garnet and the matrix are distinct, there is true dispersion of the individual ages within each of the two populations that span nearly 50 Ma. The individual zircon ages and trace element chemistry variations with age may therefore imply that protracted zircon growth in sample EA records a significant portion of the early Franciscan subduction history.

6. Conclusions

Early onset of Franciscan subduction began no later than approximately 180 Ma. Franciscan subduction metamorphism was continuous for approximately 100 Ma, suggesting that the Franciscan was a single and long-lived subduction zone. Sample EA is unique in containing two populations of zircon within a single sample that record distinct eclogite and amphibolite metamorphic events. The dispersion of zircon ages within each of these populations mirrors the age distribution of high-grade blocks throughout the Franciscan Complex. The occurrence of eclogite and amphibolite high-grade blocks throughout much of the early

Franciscan subduction history and the occurrence of both clockwise and counterclockwise pressure-temperature paths must reflect a variety of mechanisms that operated at different times, geographic locations, and depths within the subduction zone. The oldest eclogite and amphibolite ages within the Franciscan Complex predate the formation of the Coast Range Ophiolite and support tectonic models that place the ophiolite above an east dipping Franciscan subduction zone.

Acknowledgments

We thank Nicholas Botto and Sarah Roeske at U. C. Davis for their assistance with the electron microprobe and Diane Wilford and Charles Knack at WSU for their assistance with isotope geochemistry and mass spectrometry, respectively. We thank Chris Mattinson and Alexis Plunder for their helpful and constructive reviews and John Geissman for his editorial handling of the manuscript. Funding for this work was provided by U. C. Davis to H. W. Day, the U. C. Davis Cordell Durrell Fund to J. K. Starnes, and by NSF-EAR grants 1119237 and 1119247 to S. R. Mulcahy and J. D. Vervoort, respectively. Data from this study are available in the supporting information and deposited in a digital repository at <http://doi.org/10.5281/zenodo.1161276> (Mulcahy et al., 2018).

References

- Anczkiewicz, R., Platt, J. P., Thirwall, M. F., & Wakabayashi, J. (2004). Franciscan subduction off to a slow start: Evidence from high-precision Lu-Hf garnet ages on high grade-blocks. *Earth and Planetary Science Letters*, 225(1-2), 147–161. <https://doi.org/10.1016/j.epsl.2004.06.003>
- Awalt, M. B., Page, F. Z., Walsh, E. O., Kylander-Clark, A., & Wirth, K. R. (2013). New evidence for old subduction in the Catalina schist, Catalina Island, CA. *Geological Society of America Abstracts and Programs*, 47, 798.
- Bailey, E. H., Blake, M. C., & Jones, D. L. (1970). On-land Mesozoic oceanic crust in California coast ranges. *U.S. Geological Survey Professional Paper*, 700, C70–C81.
- Bebout, G. E., & Penniston-Dorland, S. C. (2016). Fluid and mass transfer at subduction interfaces—The field metamorphic record. *Lithos*, 240–243, 228–258. <https://doi.org/10.1016/j.lithos.2015.10.007>
- Bero, D. (2014). Geology of Ring Mountain and Tiburon Peninsula, Marin County, California, *California Geological Survey Map Sheet 60 Text Scales 1 12000 1 6000 2 Sheets*.
- Borg, I. Y. (1956). Glaucophane schists and eclogites near Healdsburg, California. *Geological Society of America Bulletin*, 67(12), 1563–1584. [https://doi.org/10.1130/0016-7606\(1956\)67%5B1563:GSAENH%5D2.0.CO;2](https://doi.org/10.1130/0016-7606(1956)67%5B1563:GSAENH%5D2.0.CO;2)
- Brothers, R. N. (1954). Glaucophane schists from the North Berkeley Hills, California. *American Journal of Science*, 252(10), 614–626. <https://doi.org/10.2475/ajs.252.10.614>
- Catlos, E. J., & Sorensen, S. S. (2003). Phengite-based chronology of K- and Ba-rich fluid flow in two paleosubduction zones. *Science*, 299(5603), 92–95. <https://doi.org/10.1126/science.1076977>
- Cloos, M. (1985). Thermal evolution of convergent plate margins: Thermal modeling and reevaluation of isotopic Ar-ages for blueschists in the Franciscan Complex of California. *Tectonics*, 4(5), 421–433. <https://doi.org/10.1029/TC0041005p00421>
- Coleman, R. G., & Lanphere, M. A. (1971). Distribution and age of high-grade blueschists, associated eclogites and amphibolites from Oregon and California. *Geological Society of America Bulletin*, 82(9), 2397–2412. [https://doi.org/10.1130/0016-7606\(1971\)82%5B2397:DAAOHB%5D2.0.CO;2](https://doi.org/10.1130/0016-7606(1971)82%5B2397:DAAOHB%5D2.0.CO;2)
- Conover, W. J. (1971). *Practical nonparametric statistics*. New York: John Wiley & Sons.
- Cruz-Uribe, A. M., & Feineman, M. D. (2009). Detailed geochemical analysis of a garnetite vein in eclogite, Ring Mountain, CA, AGU Fall Meeting Abstracts.
- Cruz-Uribe, A. M., & Feineman, M. D. (2010). REE mobility in subduction fluids; an example from Franciscan eclogite. *Geochimica et Cosmochimica Acta*, 74(12), A198.
- Dalrymple, G. B. (1979). Critical tables for conversion of K-Ar ages from old to new constants. *Geology*, 7(11), 558–560. [https://doi.org/10.1130/0091-7613\(1979\)7%3C558:CTFCOK%3E2.0.CO;2](https://doi.org/10.1130/0091-7613(1979)7%3C558:CTFCOK%3E2.0.CO;2)
- Daniel, W. W. (1990). *Applied nonparametric statistics*. Boston, MA: PWS-Kent Publ.
- Day, H. W., & Bickford, M. (2004). Tectonic setting of the Jurassic Smartville and Slate Creek complexes, northern Sierra Nevada, California. *Geological Society of America Bulletin*, 116(11–12), 1515–1528. <https://doi.org/10.1130/B25416.1>
- Day, H. W., Blake, M. C., Ernst, W. G., Hacker, B. R., Howard, K., Jacobson, C. J., et al. (2003). A preliminary metamorphic map of California. In *Geological Society of America Abstracts with Programs* (Vol. 35, p. 96).
- Dickinson, W. R. (1970). Relations of andesites, granites, and derivative sandstones to arc-trench tectonics. *Reviews of Geophysics*, 8(4), 81–860.
- Dickinson, W. R., Schweickert, R. A., & Ingersoll, R. D. (1996). Coast range ophiolite as backarc/interarc basin lithosphere. *GSA Today*, 6(2), 2–3.
- Dumitru, T. A., Wakabayashi, J., Wright, J. E., & Wooden, J. L. (2010). Early Cretaceous Transition from Nonaccretionary Behavior to Strongly Accretionary Behavior within the Franciscan Subduction Complex. *Tectonics*, 29, TC5001. <https://doi.org/10.1029/2009TC002542>
- Ernst, W. G. (1970). Tectonic contact between the Franciscan mélange and the Great Valley Sequence—crustal expression of a late Mesozoic benioff zone. *Journal of Geophysical Research*, 75(5), 886–901. <https://doi.org/10.1029/JB075i005p00886>
- Ernst, W. G. (2015). Franciscan geologic history constrained by tectonic/olistostromal high-grade metamafic blocks in the iconic California Mesozoic-Cenozoic accretionary complex. *American Mineralogist*, 100(1), 6–13. <https://doi.org/10.2138/am-2015-4850>
- Evarts, R. C., Sharp, W. D., & Phelps, D. W. (1992). The Del Puerto canyon remnant of the Great Valley ophiolite: Geochemical and age constraints on its formation and evolution. *Bulletin of the American Association of Petroleum Geologists*, 76, 418.
- Fagan, T. J., Day, H. W., & Hacker, B. R. (2001). Timing of arc construction and metamorphism in the Slate Creek complex, northern Sierra Nevada, California. *Geological Society of America Bulletin*, 113(8), 1105–1118. [https://doi.org/10.1130/0016-7606\(2001\)1132.0.CO;2](https://doi.org/10.1130/0016-7606(2001)1132.0.CO;2)
- Firsov, L. V., & Dobretsov, N. L. (1970). Age of glaucophane metamorphism at the northwestern fringe of the Pacific Ocean. *Doklady Akademii Nauk SSSR*, 185, 46–48.
- Fritz, D. M. (1975). *Ophiolite Belt West of Paskenta, Northern California Coast Range*. Austin TX: University of Texas at Austin.
- Gerya, T. V., Stöckhert, B., & Perchuk, A. L. (2002). Exhumation of high-pressure metamorphic rocks in a subduction channel: A numerical simulation. *Tectonics*, 21(6), 1056. <https://doi.org/10.1029/2002TC001406>
- Godfrey, N. J., & Klemperer, S. L. (1998). Ophiolitic basement to a forearc basin and implications for continental growth: The coast range/Great Valley ophiolite, California. *Tectonics*, 17(4), 558–570. <https://doi.org/10.1029/98TC01536>
- Hacker, B. R. (1993). Evolution of the northern Sierra Nevada metamorphic belt: Petrological, structural, and Ar/Ar constraints. *Geological Society of America Bulletin*, 105(5), 637–656. [https://doi.org/10.1130/0016-7606\(1993\)105%3C0637:EOTNSN%3E2.3.CO;2](https://doi.org/10.1130/0016-7606(1993)105%3C0637:EOTNSN%3E2.3.CO;2)
- Hamilton, W. (1969). Mesozoic California and the underflow of Pacific mantle. *Geological Society of America Bulletin*, 80(12), 2409–2430. [https://doi.org/10.1130/0016-7606\(1969\)80%5B2409:MCATUO%5D2.0.CO;2](https://doi.org/10.1130/0016-7606(1969)80%5B2409:MCATUO%5D2.0.CO;2)
- Hopson, C. A., Mattinson, J. M., & Pessagno, E. A. (1981). Coast Range Ophiolite, western California. In W. G. Ernst (Ed.), *The geotectonic development of California*, Vol. Rubey (Vol. 1, pp. 418–510). Englewood Cliffs, NJ: Prentice-Hall.
- Hopson, C. A., Mattinson, J. M., Pessagno, E. A., & Luyendyk, B. P. (2008). California Coast Range Ophiolite: Composite Middle And Late Jurassic oceanic lithosphere. In J. E. Wright & J. W. Shervais (Eds.), *Ophiolites, arcs and batholiths: A tribute to Cliff Hopson*, *Geological Society of America Special Paper* (Vol. 438, pp. 1–102). Boulder, CO: Geological Society of America. [https://doi.org/10.1130/2008.2438\(01\)](https://doi.org/10.1130/2008.2438(01))

- Hopson, C. A., Pessagno, E. A. Jr., Mattinson, J. M., Luyendyk, B. P., Beebe, W., Hull, D. M., et al. (1996). Coast Range Ophiolite as paleoequatorial mid-ocean lithosphere. *GSA Today*, 6(2), 3–4.
- Ingersoll, R. V., & Schweickert, R. A. (1986). A plate-tectonic model for Late Jurassic ophiolite genesis, Nevadan orogeny and forearc initiation, northern California. *Tectonics*, 5(6), 901–912. <https://doi.org/10.1029/TC005i06p00901>
- Joesten, R., Wooden, J. L., Silver, L. T., Ernst, W. G., & McWilliams, M. O. (2004). Depositional age and provenance of jadeite-grade metagraywacke from the accretionary prism, Diablo range, central California-SHRIMP Pb-isotope dating of detrital zircon. *Geological Society of America Abstracts with Programs*, 36, 120.
- Keith, T. E. C., & Coleman, R. G. (1968). Albite-pyroxene-glaucophane schist from Valley Ford, California. *U.S. Geological Survey Professional Paper*, 600C, C13–C17.
- Krogh, E. J., Oh, C. W., & Liou, J. C. (1994). Polyphase and anticlockwise P-T evolution for Franciscan eclogites and blueschists from Jenner, California, USA. *Journal of Metamorphic Geology*, 12(2), 121–134. <https://doi.org/10.1111/j.1525-1314.1994.tb00008.x>
- Lanphere, M. A. (1971). Age of Mesozoic oceanic crust in the California Coast Ranges. *Geological Society of America Bulletin*, 82(11), 3209–3212. [https://doi.org/10.1130/0016-7606\(1971\)82%5B3209:AOTMOC%5D2.0.CO;2](https://doi.org/10.1130/0016-7606(1971)82%5B3209:AOTMOC%5D2.0.CO;2)
- Lanphere, M. A., Blake, M. C., & Irwin, W. P. (1978). Early Cretaceous metamorphic age of the South Fork Mountain schist in the northern Coast Ranges of California. *American Journal of Science*, 278(6), 798–815. <https://doi.org/10.2475/ajs.278.6.798>
- Leake, B. E., Woolley, A. R., Arps, C. E., Birch, W. D., Gilbert, M. C., Grice, J. D., et al. (1997). Nomenclature of amphiboles: Report of the subcommittee on amphiboles of the International Mineralogical Association, commission on new minerals and mineral names. *American Mineralogist*, 82(9–10), 1019–1037.
- Lee, D. E., Thomas, H. H., Marvin, R. F., & Coleman, R. G. (1964). Isotopic ages of glaucophane schists from the area of Cazadero, California. *U.S. Geological Survey Professional Paper*, 475–D, D105–D107.
- Ludwig, K. (2009). Isoplot: A geochronological toolkit for Microsoft Excel. *Berkeley Geochronology Center Special Publication*, 4, 70.
- Mahon, K. L. (1996). The New “York” regression: Application of an improved statistical method to geochemistry. *International Geologic Review*, 38(4), 293–303. <https://doi.org/10.1080/00206819709465336>
- Mankinen, E. A., Gromme, C. S., & Williams, K. M. (1991). Concordant paleolatitudes from ophiolite sequences in the northern California Coast Ranges, U. S. A. *Tectonophysics*, 198(1), 1–21. [https://doi.org/10.1016/0040-1951\(91\)90127-E](https://doi.org/10.1016/0040-1951(91)90127-E)
- Mattinson, J. M. (1986). Geochronology of high-pressure-low-temperature Franciscan metabasites: A new approach using the U-Pb system. *Geological Society of America Memoirs*, 164, 95–105. <https://doi.org/10.1130/MEM164-p95>
- Mattinson, J. M., & Echeverria, L. M. (1980). Ortigalita Peak gabbro, Franciscan Complex: U-Pb dates of intrusion and high-pressure-low-temperature metamorphism. *Geology*, 8(12), 589–593. [https://doi.org/10.1130/0091-7613\(1980\)8%3C589:opgfcu%3E2.0.co;2](https://doi.org/10.1130/0091-7613(1980)8%3C589:opgfcu%3E2.0.co;2)
- Mattinson, J. M., & Hill, D. J. (1976). Age of plutonic basement rocks, Santa Cruz Island, California. In D. G. Howell (Ed.), *Aspects of the geologic history of the California continental borderland*, *Miscellaneous Publication* (Vol. 24, pp. 53–58). Menlo Park: American Association of Petroleum Geologists. Pacific Section.
- Mattinson, J. M., & Hopson, C. A. (2008). New high-precision CA-TIMS U-Pb zircon plateau ages for the Point Sal and San Simeon ophiolite remnants, California Coast Ranges. In J. E. Wright & J. W. Shervais (Eds.), *Ophiolites, arcs and batholiths: A tribute to Cliff Hopson*, *Geological Society of America Special Paper* (Vol. 438, pp. 103–112). Boulder, CO: Geological Society of America. [https://doi.org/10.1130/2008.2438\(02\)](https://doi.org/10.1130/2008.2438(02))
- McDonough, W. F., & Sun, S. S. (1995). The composition of the Earth. *Chemical Geology*, 120(3–4), 223–253. [https://doi.org/10.1016/0009-2541\(94\)00140-4](https://doi.org/10.1016/0009-2541(94)00140-4)
- McDowell, F. W., Lehman, D. H., Gucwa, P. R., Fritz, D., & Maxwell, J. C. (1984). Glaucophane schists and ophiolites of the northern California Coast Ranges: Isotopic ages and their tectonic implications. *Geological Society of America Bulletin*, 95(11), 1373–1382. [https://doi.org/10.1130/0016-7606\(1984\)95%3C1373:GSAOOT%3E2.0.CO;2](https://doi.org/10.1130/0016-7606(1984)95%3C1373:GSAOOT%3E2.0.CO;2)
- McLaughlin, R. J., & Ohlin, H. N. (1984). Tectonostratigraphic framework of the Geysers-Clear Lake region, California. In M. C. Blake (Ed.), *Franciscan geology of northern California* (Vol. 43, pp. 221–254). Los Angeles, CA: Pacific Section, Society of Economic Paleontologists and Mineralogists.
- Moore, D. E., & Blake, M. C. (1989). New evidence for polyphase metamorphism of glaucophane schist and eclogite exotic blocks in the Franciscan Complex, California and Oregon. *Journal of Metamorphic Geology*, 7, 211–228.
- Mulcahy, S. R., King, R. L., & Vervoort, J. D. (2009). Lawsonite Lu-Hf geochronology: A new geochronometer for subduction zone processes. *Geology*, 37(11), 987–990. <https://doi.org/10.1130/G30292A.1>
- Mulcahy, S. R., Starnes, J. K., Day, H. W., Coble, M. C., Vervoort, J. D., & Vervoort, J. D. (2018). Data and code to accompany the manuscript early onset of Franciscan subduction (version 1.0). *Tectonics*, 37. <https://doi.org/10.5281/zenodo.1161276>
- Mulcahy, S. R., Vervoort, J. D., & Renne, P. R. (2014). Dating subduction-zone metamorphism with combined garnet and lawsonite Lu-Hf geochronology. *Journal of Metamorphic Geology*, 32(5), 515–533. <https://doi.org/10.1111/jmg.12092>
- Oh, C. W., & Liou, J. G. (1990). Metamorphic evolution of two different eclogites in the Franciscan Complex, California, USA. *Lithos*, 25(1–3), 41–53. [https://doi.org/10.1016/0024-4937\(90\)90005-L](https://doi.org/10.1016/0024-4937(90)90005-L)
- Page, F. Z., Essene, E. J., Mukasa, S. B., & Valley, J. W. (2013). A garnet-zircon oxygen isotope record of subduction and exhumation fluids from the Franciscan Complex, California. *Journal of Petrology*, 55(1), 103–131. <https://doi.org/10.1093/petrology/egt062>
- Page, F. Z., Lora, S. A., Eric, J. E., & Samuel, B. M. (2007). Prograde and retrograde history of the Junction School eclogite, California, and an evaluation of garnet-phengite-clinopyroxene thermobarometry. *Contributions to Mineralogy and Petrology*, 153(5), 533–555. <https://doi.org/10.1007/s00410-006-0161-9>
- Page, F. Z., Mukasa, S. B., Essene, E. J., & Carrigan, C. W. (2003). Lu-Hf and U-Pb chronology of a possible Triassic high-grade block, Healdsburg, California. *Eos, Transactions of the American Geophysical Union*, 84, F1567.
- Peterman, Z. E., Hedge, C. E., Coleman, R. G., & Snively, P. D. (1967). ⁸⁷Sr/⁸⁶Sr ratios in some eugeosynclinal sedimentary rocks and their bearing on the origin of granitic magma in orogenic belts. *Earth and Planetary Science Letters*, 2(5), 433–439. [https://doi.org/10.1016/0012-821X\(67\)90185-9](https://doi.org/10.1016/0012-821X(67)90185-9)
- Platt, J. P. (1975). Metamorphic and deformational processes in the Franciscan Complex, California: Some insights from the Catalina Schist terrane. *Geological Society of America Bulletin*, 96, 1337–1347.
- Ross, J. A., & Sharp, W. D. (1986). ⁴⁰Ar/³⁹Ar and Sm/Nd dating of garnet amphibolite in the Coast Ranges, California. *Eos, Transactions of the American Geophysical Union*, 67, 1249.
- Ross, J. A., & Sharp, W. D. (1988). The effects of sub-blocking temperature metamorphism on the K/Ar systematics of hornblendes: ⁴⁰Ar/³⁹Ar dating of polymetamorphic garnet amphibolite from the Franciscan Complex, California. *Contributions to Mineralogy and Petrology*, 100(2), 213–221. <https://doi.org/10.1007/BF00373587>
- Rubatto, D. (2002). Zircon trace element geochemistry: Partitioning with garnet and the link between U–Pb ages and metamorphism. *Chemical Geology*, 184(1–2), 123–138. [https://doi.org/10.1016/S0009-2541\(01\)00355-2](https://doi.org/10.1016/S0009-2541(01)00355-2)

- Saleeby, J. B. (1996). Coast Range ophiolite as parautochthonous forearc lithosphere. *GSA Today*, 6(2), 6–9.
- Scherer, E., Münker, C., & Mezger, K. (2001). Calibration of the lutetium-hafnium clock. *Science*, 293(5530), 683–687. <https://doi.org/10.1126/science.1061372>
- Shervais, J. W., Murchey, B. L., Kimbrough, D. L., Renne, P. R., & Hanan, B. (2005). Radioisotopic and biostratigraphic age relations in the Coast Range Ophiolite, northern California: Implications for the tectonic evolution of the Western Cordillera. *Geological Society of America Bulletin*, 117(5), 633–653. <https://doi.org/10.1130/B25443.1>
- Skublov, S., Berezin, A., & Berezhnaya, N. (2012). General relations in the trace-element composition of zircons from eclogites with implications for the age of eclogites in the Belomorian Mobile Belt. *Petrology*, 20(5), 427–449. <https://doi.org/10.1134/S0869591112050062>
- Söderlund, U., Patchett, P. J., Vervoort, J. D., & Isachsen, C. E. (2004). The 176 Lu decay constant determined by Lu–Hf and U–Pb isotope systematics of Precambrian mafic intrusions. *Earth and Planetary Science Letters*, 219(3–4), 311–324. [https://doi.org/10.1016/S0012-821X\(04\)00012-3](https://doi.org/10.1016/S0012-821X(04)00012-3)
- Sorensen, S., & Grossman, J. (1989). Enrichment of trace elements in garnet amphibolites from a paleo-subduction zone: Catalina schist, southern California. *Geochimica et Cosmochimica Acta*, 53(12), 3155–3177. [https://doi.org/10.1016/0016-7037\(89\)90096-3](https://doi.org/10.1016/0016-7037(89)90096-3)
- Starnes, J. K. (2014). *Multi-stage metamorphism of amphibolite in Franciscan mélange*. Davis: Ring Mountain, California, University of California.
- Stern, R. J., & Bloomer, S. H. (1992). Subduction zone infancy: Examples from the Eocene Izu-Bonin-Mariana and Jurassic California arcs. *Geological Society of America Bulletin*, 104(12), 1621–1636. [https://doi.org/10.1130/0016-7606\(1992\)104%3C1621:SZIEFT%3E2.3.CO;2](https://doi.org/10.1130/0016-7606(1992)104%3C1621:SZIEFT%3E2.3.CO;2)
- Suppe, J. (1969). Times of metamorphism in the Franciscan terrain of the northern Coast Ranges, California. *Geological Society of America Bulletin*, 80(1), 135–142. [https://doi.org/10.1130/0016-7606\(1969\)80%5B135:TOMITF%5D2.0.CO;2](https://doi.org/10.1130/0016-7606(1969)80%5B135:TOMITF%5D2.0.CO;2)
- Suppe, J., & Armstrong, R. L. (1972). Potassium-argon dating of Franciscan metamorphic rocks. *American Journal of Science*, 272(3), 217–233. <https://doi.org/10.2475/ajs.272.3.217>
- Suppe, J., & Foland, K. A. (1978). The Goat Mountain schists and Pacific Ridge complex: A reformed but still-intact late Mesozoic Franciscan schuppen complex. In D. G. Howell & K. McDougall (Eds.), *Pac. Coast Paleogeography Symposium* (pp. 431–451). Pacific Section, Society of Economic Paleontologists and Mineralogists.
- Switzer, G. S. (1945). Eclogite from the California glaucophane schists. *American Journal of Science*, 243(1), 1–8. <https://doi.org/10.2475/ajs.243.1.1>
- Tripathy, A., Housh, T. B., Morisani, A. M., & Cloos, M. (2005). Detrital zircon geochronology of coherent pyroxene-bearing rocks of the Franciscan Complex, Pacheco Pass, California: Implications for unroofing. *Geological Society of America Abstracts and Programs*, 37, 18.
- Tsujimori, T., Matsumoto, K., Wakabayashi, J., & Liou, J. G. (2006). Franciscan eclogite revisited: Reevaluation of the P-T evolution of tectonic blocks from Tiburon Peninsula, California, U.S.A. *Mineralogy and Petrology*, 88(1–2), 243–267. <https://doi.org/10.1007/s00710-006-0157-1>
- Ukar, E. (2012). Tectonic significance of low-temperature blueschist blocks in the Franciscan mélange at San Simeon, California. *Tectonophysics*, 568–569, 154–169. <https://doi.org/10.1016/j.tecto.2011.12.039>
- Ukar, E., & Cloos, M. (2014). Low-temperature blueschist-facies mafic blocks in the Franciscan mélange, San Simeon, California: Field relations, petrology, and counterclockwise PT paths. *Geological Society of America Bulletin*, 126(5–6), 831–856. <https://doi.org/10.1130/B30876.1>
- Ukar, E., Cloos, M., & Vasconcelos, P. (2012). First $^{40}\text{Ar}/^{39}\text{Ar}$ ages from low-T mafic blueschist blocks in a Franciscan mélange near San Simeon: Implications for initiation of subduction. *Journal of Geology*, 120(5), 543–556. <https://doi.org/10.1086/666745>
- Unruh, J. R., Dumitru, T. A., & Sawyer, T. L. (2007). Coupling of early Tertiary extension in the Great Valley forearc basin with blueschist exhumation in the underlying Franciscan accretionary wedge at Mount Diablo, California. *Geological Society of America Bulletin*, 119(11–12), 1347–1367. <https://doi.org/10.1130/b26057.1>
- Wakabayashi, J. (1990). Counterclockwise P-T-t paths from amphibolites, Franciscan Complex, California: Relics from the early stages of subduction zone metamorphism. *Journal of Geology*, 98(5), 657–680. <https://doi.org/10.1086/629432>
- Wakabayashi, J. (1992). Nappes, tectonics of oblique plate convergence, and metamorphic evolution related to 140 million years of continuous subduction, Franciscan Complex, California. *Journal of Geology*, 100(1), 19–40. <https://doi.org/10.1086/629569>
- Wakabayashi, J., & Deino, A. (1989). Laser-probe $^{40}\text{Ar}/^{39}\text{Ar}$ ages from high grade blocks and coherent blueschists, Franciscan Complex, California: Preliminary results and implications for Franciscan tectonics. *Geological Society of America Abstracts and Programs*, 21, A267.
- Wakabayashi, J., & Dumitru, T. A. (2007). $^{40}\text{Ar}/^{39}\text{Ar}$ ages from coherent, high-pressure metamorphic rocks of the Franciscan Complex, California: Revisiting the timing of metamorphism of the world's type subduction complex. *International Geology Review*, 49(10), 873–906. <https://doi.org/10.2747/0020-6814.49.10.873>
- Wendt, I., & Carl, C. (1991). The statistical distribution of the mean squared weighted deviation. *Chemical Geology*, 86(4), 275–285. [https://doi.org/10.1016/0168-9622\(91\)90010-T](https://doi.org/10.1016/0168-9622(91)90010-T)
- Wright, J. E., & Fahan, M. R. (1988). An expanded view of Jurassic orogenesis in the western United States Cordillera: Middle Jurassic (pre-Nevadan) regional metamorphism and thrust faulting within an active arc environment, Klamath Mountains, California. *Geological Society of America Bulletin*, 100(6), 859–876. [https://doi.org/10.1130/0016-7606\(1988\)100%3C0859:AEVOJO%3E2.3.CO;2](https://doi.org/10.1130/0016-7606(1988)100%3C0859:AEVOJO%3E2.3.CO;2)